Electrochimica Acta 526 (2025) 146087

Contents lists available at ScienceDirect

Electrochimica Acta

journal homepage: www.journals.elsevier.com/electrochimica-acta

Lithium-ion battery separators based on sustainable collagen and chitosan hybrid membranes

Mireia Andonegi [a,b,*], João P. Serra [b], Maria M. Silva [c], Renato Gonçalves [c], Carlos M. Costa [b,d], Senentxu Lanceros-Mendez [b,e,f], Koro de la Caba [a,e,*], Pedro Guerrero [a,e,g]

[a] BIOMAT Research Group, University of the Basque Country (UPV/EHU), Escuela de Ingeniería de Gipuzkoa, Plaza de Europa 1, 20018 Donostia-San Sebastián, Spain
[b] Physics Centre of Minho and Porto Universities (CF-UM-UP) and Laboratory of Physics for Materials and Emergent Technologies, LapMET, University of Minho 4710-057 Braga, Portugal
[c] Centre of Chemistry, University of Minho, 4710-057 Braga, Portugal
[d] Institute of Science and Innovation for Bio-Sustainability (IB-S), University of Minho, 4710-053 Braga, Portugal
[e] BCMaterials, Basque Center for Materials, Applications and Nanostructures, UPV/EHU Science Park, 48940 Leioa, Spain
[f] Ikerbasque, Basque Foundation for Science, 48009 Bilbao, Spain
[g] Proteinmat materials SL, Avenida de Tolosa 72, 20018 Donostia-San Sebastián, Spain

ARTICLE INFO

Keywords:
Collagen
Chitosan
Porous membranes
Lithium-ion batteries

ABSTRACT

This work focuses on the production of sustainable membranes based on collagen and chitosan as separators in lithium-ion batteries. Membranes were prepared by freeze-drying with varying collagen and chitosan contents. All membranes show interconnected pores with different pore sizes and porosity above 90 %, allowing high values of electrolyte uptake. As for thermal and mechanical characteristics, the addition of chitosan improves both thermal and mechanical stability. After 1 M $LiPF_6$ in EC:DMC electrolyte uptake, the ionic conductivity is above 0.49 $mS{\cdot}cm^{-1}$ for all membranes and is most affected by the collagen content. Furthermore, the membranes present a lithium transfer number value of 0.2. In cathodic half-cells with $LiFePO_4$, the obtained room temperature discharge capacity is above 140 $mAh{\cdot}g^{-1}$ at C/8 rate. For high C rates (C and 2C rates), the membranes with 80 wt % of collagen and 20 wt % of chitosan present 42 $mAh{\cdot}g^{-1}$ after 100 cycles at C rate, demonstrating adequate reversibility. Considering the need for more environmentally friendly materials and methods compatible with a circular economy, the bio-based membranes developed in this work constitute an alternative for synthetic separators.

1. Introduction

Energy and environment rank among the most pressing global challenges of our time [1]. In this scope and based on the strategy to reduce carbon emissions by 2050, it is necessary to reduce dependence on fossil fuels. Thus, renewable energy sources such as photovoltaic, hydro, and wind power will need to be implemented on a large scale in a scenario of increasing global energy demand [2], being also necessary their coupling to energy storage systems (ESS), based on their intermittent nature [3,4].

Batteries are electrochemical systems based on oxidation–reduction reactions that convert chemical energy into electrical energy and vice versa [5]. The first batteries were developed in the 18th century when Alessandro Volta invented the voltaic pile [6], but batteries began to gain great relevance in 1991 with the development of lithium-ion batteries (LIBs), that have been increasingly implemented in portable electronic as well as in electric vehicles [2,7]. When compared with other battery technologies, LIBs emerge as the lighter and more cost-effective option, offering higher energy density, reduced self-discharge, absence of memory effects, extended service life, and a large number of charge/discharge cycles [8–10]. Currently, LIBs reign supreme among energy storage systems, boasting a compound annual growth rate (CAGR) of 17.0 % and an anticipated global market value of USD $93.1 billion by 2025 [8].

Among the different battery components, the separator is defined as a membrane saturated in an electrolyte solution (separator), which separated the electrodes (anode and cathode) [11]. It is classified as an inactive cell component, but it is a critical component in LIBs as its

* Corresponding authors.
E-mail addresses: mireia.andonegui@ehu.es (M. Andonegi), koro.delacaba@ehu.es (K. de la Caba).

https://doi.org/10.1016/j.electacta.2025.146087
Received 18 December 2024; Received in revised form 18 February 2025; Accepted 19 March 2025
Available online 11 April 2025
0013-4686/© 2025 The Authors. Published by Elsevier Ltd. This is an open access article under the CC BY license (http://creativecommons.org/licenses/by/4.0/).

properties considerably affect the overall battery performance, affecting ion mobility, cycle life and safety. The separator allows the diffusion of lithium ions through it but also prevents the contact between the two electrodes, avoiding short circuit [12]. Consequently, separators must exhibit electronic insulation [13] and must display high ionic conductivity either by intrinsic ionic conduction or by soaking an electrolyte. It is also required to be corrosive-resistant to organic solvents, as they are often involved in the electrolytes used in rechargeable battery system. Furthermore, this material should ideally be highly resistant to the electrochemical processes from electrodes and electrolyte and protect against short circuit, thermal runaway and overcharge. So, they must present complementary important characteristics for a correct battery operation, such as mechanical, thermal, chemical, and electrical stability, porous morphology, suitable wettability by the electrolyte, and resistance to electrochemical degradation [14,15].

The growing global demand for energy storage technologies has increased the need for materials that not only meet the performance criteria of highly efficient energy storage systems, but also adhere to sustainability principles [16]. Most of the materials used in battery separators, such as poly(acrylonitrile) (PAN), poly(ethylene oxide) (PEO), poly(ethylene) (PE), poly(propylene) (PP), and poly(vinylidene fluoride) (PVDF), are often products resulting from the transformation of fossil fuels [13]. Achieving sustainability in the realm of batteries can be complex, but it starts with replacing some of these materials by sustainable ones. Within this framework, polymers derived from biomass assume particular significance due to their abundance, compatibility with cost-effective processing techniques, and alignment with the principles of circular economy and sustainable development [17]. Some of these biopolymers have already begun to find application as battery separators, such as cellulose and its derives [18], yielding promising outcomes. Within the various sustainable materials, collagen can also be considered as an alternative to conventional synthetic polymers used in LIBs. Collagen has the advantages of being sustainable, environmentally friendly, renewable and degradable [19]. In terms of chemical structure, the collagen backbone is composed by three parallel polypeptide-alpha chains in the form of cross-linked fibrils with a triple helix structure that leads to the formation of insoluble fibers responsible for the high mechanical strength and integrity of the extracellular matrix of mammalians [20]. However, collagen, while a promising material for battery separator applications, does come with certain limitations. One of its main drawbacks is its relatively low thermal stability, which can make it susceptible to thermal degradation in high-temperature environments [21]. Additionally, collagen may not exhibit the desired level of resistance to moisture or ionic conductivity required for efficient battery separators. Chitosan, a polycationic polymer obtained by the deacetylation of chitin [22], on the other hand, offers solutions to these challenges. Chitosan can enhance the thermal stability of collagen-based separators, making them more resilient to temperature fluctuations [23]. Its inherent moisture resistance properties also aid in maintaining the separator's integrity in humid conditions. Moreover, chitosan contributes to improved ionic conductivity, essential for battery performance [24]. Furthermore, both collagen and chitosan can show a good electrochemical stability, mainly because the amino and hydroxyl groups in the chitosan and collagen could function as Lewis bases to react with the Lewis acid produced by electrolyte decomposition, slowing the electrolyte decomposition [25]. By combining collagen and chitosan, it is possible to obtain separators that mitigate these drawbacks and provide a more effective and reliable solution for battery applications.

In this context, the objective of this work is to develop LIB separators based on natural materials for a new generation of sustainable batteries. Separators based on collagen with different amounts of chitosan and different porosity were developed through a freeze-drying process, and the influence of chitosan content and porosity on separator membranes was evaluated through their morphological, crystallographic, thermal, physicochemical and mechanical properties. The developed membranes were also tested for battery applications by assessing electrolyte uptake, ionic conductivity and lithium transfer number, as well as charge-discharge half-cell battery tests. Furthermore, this work is related to the valorization of residual biomass or by-products from industry, rich in proteins and polysaccharides, which can represent a worthy approach to prepare sustainable battery components. Taking all this into account, the evaluation of chitosan/collagen membranes as battery separators is the main goal of this work, which aims to support the development of sustainable separators for the future.

2. Materials and methods

2.1. Materials

Collagen was supplied by Proteinmat materials S.L. (Spain). Chitosan (batch MKBB9037) with a molecular weight of 190 kDa and a degree of deacetylation higher than 75 %, lithium hexafluorophosphate ($LiPF_6$) in a mixture of ethyl carbonate (EC) and dimethyl carbonate (DMC) (1:1 in vol. ratio), N-methyl-2-pyrrolidone (NMP) and metallic lithium were provided by Sigma-Aldrich (Spain). Acetic acid and ethanol were supplied by Panreac Quimica S.L.U (Spain). Poly(vinylidene fluoride) (PVDF, Kynar PVDF HSV900), $LiFePO_4$ (LFP) and Super P conductive carbon black were purchased from Arkema (France), Phostech Lithium (Canada), and Timcal Graphite & Carbon (Switzerland), respectively.

2.2. Processing of membranes

Collagen membranes with different porosity and chitosan content (Table 1) were prepared by freeze-drying. Collagen, chitosan and 0.5 M acetic acid were mixed using an ultra-turrax T25 (IKA, Germany) until homogeneous pastes were achieved. The mixing process (2000 rpm, 2 min) was carried out in a cold bath to prevent the dough from heating up. Finally, dispersions were poured into each well of a 12 multiwell plate (Costar 3513, Corning Incorporated, USA) and the plate was freeze-dried for 48 h (Alpha 1–4 LDplus, CHRIST, Germany). Finally, cylinder-shaped collagen-chitosan samples (2.26 cm diameter and 1 cm height) were taken out from the wells.

In the following, the membranes are designated, with the first number being the concentration of collagen in the acetic acid solution for control samples or the concentration of both biopolymers (chitosan and collagen) in the acetic acid solution for collagen-chitosan membranes, and the last number being the chitosan (CHI) content with respect to total biopolymer mass. The control represents the membrane with collagen only.

2.3. Physicochemical characterization

The morphology of the membranes was analyzed by field emission scanning electron microscopy (SEM), Hitachi S-4800 (Hitachi High-Technologies Corporation, Japan), at an acceleration voltage of 15 kV. Samples were mounted on a metal stub with double-side adhesive tape and coated under vacuum with a JEOL fine-coat ion sputter JFC-1100 (Izasa, Spain) in an argon atmosphere prior to observation. SEM images were analyzed by ImageJ software for pore size evaluation.

To assess the porosity of the specimens, the pycnometry method was

Table 1
Composition of the freeze-dried membranes.

Samples	Concentration of biopolymers in solution (%)	Collagen (% w/w)	Chitosan (% w/w)
3Control	3	100	0
3CHI20	3	80	20
3CHI40	3	60	40
7Control	7	100	0
7CHI20	7	80	20
7CHI40	7	60	40

employed. The procedure entailed several steps. Initially, the weight of the pycnometer filled with ethanol was measured and labeled as W_1. Next, the sample, having a known weight, W_s, was immersed in the ethanol contained within the pycnometer. Care was taken to ensure that the pores within the membranes were fully saturated with ethanol. Additional ethanol was then added until the pycnometer reached its maximum volume. The pycnometer was subsequently reweighed, recorded as W_2. Subsequently, the sample, now impregnated with ethanol, was carefully removed from the pycnometer. The weight of the pycnometer with the remaining weight of ethanol was noted as W_3. The porosity of the sample was determined using Eq. (1) and reported for five specimens of each sample:

$$\varepsilon\ (\%) = \frac{W_2 - W_3 - W_S}{W_1 - W_3} \times\ 100 \tag{1}$$

Fourier-transformed infrared (FTIR) spectroscopy was carried out in a ALPHA II Compact FTIR Spectrometer using attenuated total reflectance (ATR) module. A total of 32 scans were performed at 4 cm^{-1} resolution. Measurements were recorded between 4000 and 800 cm^{-1}.

Differential scanning calorimetry (DSC) was carried out in a Mettler Toledo DSC 822. Samples (3.0 ± 0.2 mg) were sealed in aluminum pans to avoid mass loss during the experiment. Filled pans were heated from 25 to 300 °C at a rate of 10 °C/min under inert atmosphere conditions (10 mL N_2/min) to avoid thermo-oxidative reactions.

X-ray diffraction (XRD) measurements were carried out at 40 kV and 40 mA, with Cu-Kα (λ = 1.5418 Å) as radiation source, using a PANalytic Xpert Pro (PANalytical, Almelo, The Netherlands) equipment with a diffraction unit. Data were collected between 2° and 50° (step size = 0.026, time per step = 118 s).

For the mechanical characterization, puncture tests were performed employing a TA.XT.Plus Texture Analyzer (Aname Instrumentación Científica). A 5 kg load cell was employed for the measurements, membranes were perforated with a spherical probe of 5 mm diameter, and data were collected at 3 mm/s speed.

2.4. Electrolyte uptake and electrochemical parameters

The membranes were immersed between 0 and 350 s in a 1 m $LiPF_6$ in EC:DMC solution and the electrolyte uptake (ELU) was calculated using Eq. (2):

$$ELU\ (\%) = \left(\frac{M - M_0}{M_0}\right) \times\ 100 \tag{2}$$

where M_0 is the membrane weight and M is the membrane weight after immersion in the electrolyte solution.

The ionic conductivity (σ_i) value of the collagen-chitosan membranes was measured using a Solartron 1260A Impedance Analyzer in a symmetric CR-2032-coin cell (Stainless-steel | separator membrane | Stainless-steel), which was assembled within an Ar-filled glovebox. The impedance tests were carried out at room temperature in a frequency range from 7×10^6 to 1 Hz and an excitation amplitude of 50 mV. Eq. (3) was used to calculate the value:

$$\sigma_i = \frac{t}{A * R_b} \tag{3}$$

where t is the thickness of the membrane, A is the area of the membrane, and R_b is the bulk resistance obtained by equivalent circuit.

The Li-ion transference number (t_{Li}^{+}) was determined by employing symmetrical lithium cells and conducting potentiostatic polarization with the application of a DC voltage of 10 mV at room temperature. The t_{Li+}value was calculated using Eq. (4):

$$t_{Li^+} = \frac{I^s\ [\Delta V - I^0 R^0]}{I^0\ [\Delta V - I^s R^s]} \tag{4}$$

where I^s and I^0 are the steady and initial currents, respectively, ΔV is the applied potential, and R^0 and R^s are the initial and final resistances of the Li electrode/electrolyte before and after polarization, respectively.

Cyclic voltammetry was used to determine the electrochemical stability of the separators in a two-electrode cell configuration (25 μm diameter gold microelectrode | separator| lithium metal). Measurements were performed in a dry argon-filled glove box at 0.01 V/s and room temperature with an Autolab PGSTAT-12 (Eco Chemie) system.

2.5. Battery preparation, assembly and characterization

The cathodic half-cells were constructed using a lithium metal | separator | LFP cathode configuration within a glovebox filled with an argon atmosphere (H_2O, O_2 < 1 ppm). Prior to assembly, both the LFP cathode material and the separator membrane were transferred into the glovebox after undergoing overnight drying at 60 °C under vacuum conditions using a Buchi TO51 tube oven. The LFP cathodes were prepared with a composition of active material:conductive material:polymer binder in a weight ratio of 80:10:10 and were deposited onto an aluminum current collector with an active mass loading of approximately 2 mg. For further details regarding the preparation process, refer to [26].

Galvanostatic charge-discharge cycles were conducted at room temperature using a Landt CT2001A instrument at various rates (C/8 = 50 μA, C/5 = 80 μA, C/2 = 200 μA, 1C = 400 μA, and 2C = 800 μA, where $C = 170\ mA{\cdot}g^{-1}$) for 10 cycles.

Impedance spectroscopy was performed before and after cycling in the batteries, employing a signal amplitude of 10 mV over a frequency range spanning from 10 mHz to 500 kHz with a Solartron 1260A Impedance Analyzer instrument.

2.6. Statistical analysis

Analysis of variance (ANOVA) was carried out with SPSS software (SPSS Statistic 25) to determine significant differences between samples. Tukey's test with a statistically significance at the $P < 0.05$ level was considered for multiple comparisons among different systems.

2.7. Environmental assessment

The environmental impact of the membranes was evaluated considering the stages of raw materials extraction, membrane manufacturing and the end-of-life scenario. SimaPro 9.6.0.1 software (Barcelona, Spain) was used in accordance with ISO 14,040 guidelines and recommendations. The Ecoinvent 3.8 database was utilized to obtain data on energy production, transport, and chemical production. The Hierarchist version of ReCiPe 2016, midpoint (H) v1.09, was employed to calculate the environmental impact.

First, the functional unit was set as 1 g of membrane. During the inventory stage, the materials used (collagen, chitosan, acetic acid, and water) and the energy (electricity) consumed were taken into account. The data associated with the extraction of collagen from bovine skins [27] and chitosan from crustracean shells [28] were sourced from previously published studies. Electricity consumption for the manufacture stage of the collagen-chitosan membranes was measured directly in the laboratory and normalized with respect to production. The main energy consumption was due to the continuous stirring of the mixture for 30 min. The impact of transport of raw materials to processing industries and from industries to consumers was not considered in this study.

3. Results and discussion

3.1. Morphology, porosity and pore size

The morphology of the membranes is an essential characteristic to be considered in battery separators, particularly in relation to pore

microstructure and connectivity. For this reason, SEM analysis of the cross-section of the samples was carried out and the images are displayed in Fig. 1. The control membrane with lower collagen concentration (3Control, Fig. 1A) showed an irregular pore structure, while the other membranes displayed high porosity and a relatively uniform and large continuous interconnected pores. The porosity (ε) of the collagen-chitosan membranes was assessed by the pycnometry method. A high porosity above 91 % was obtained for all membranes (Table 2) and this value diminishes from 97.3 ± 0.5 for 3CHI20 to 91.3 ± 1.7 for 7Control with the increase of the biopolymers concentration in the solution, primarily due to reduced water content during the freeze-drying process [29].

The resulting porous structure obtained by freeze-drying largely depends on the interaction between the components of the formulation and the processing conditions. Since all membranes obtained in this work were freeze-dried at the same time and under the same conditions, the difference in the pore structure is associated with the collagen:chitosan ratio and the polymer concentration in the solution. In this context, quantitative analysis of the pore size for each membrane was carried out and results are shown in Fig. 2.

It is observed a decrease in the average pore size and a more homogeneous structure with increasing polymer concentration in solution as well as with chitosan addition. Upon the increase in collagen concentration from 3 wt % to 7 wt %, the average pore size of the membranes decreases from 124 μm to 102 μm, due to the interaction between collagen and water. As the concentration of collagen in the solution increases, there is a larger number of collagen chains interacting with water, influencing the formation and growth of ice crystals during the freeze-drying process. This enhanced interaction between collagen and water leads to the formation of smaller pores and a more homogeneous pore distribution in the membranes [30,31]. The same trend occurs with the inclusion of chitosan in the collagen formulation, resulting in a more homogeneous porosity with some tendency for the formation of lower porous sizes [32]. Thus, the proportion of collagen and chitosan is directly related to the pore size, primarily due to molecular interactions, such as hydrogen bonding and electrostatic forces between the chitosan and collagen molecules observed by FTIR analysis (see later). Additionally, both chitosan and collagen exhibit gel-forming properties in solution, contributing to a denser and more uniform structure as water is removed during freeze-drying. This results in a more consistent distribution of smaller pores. Combining collagen and chitosan in a formulation positively affects the formation of homogeneous interconnected porous structures with smaller pores [33]. The interconnected microporous structure observed in all the samples suggests that these membranes can inhibit the formation of lithium dendrites on the graphite anode during the charging process [34]. In this context, 7CHI20 and 7CHI40 samples are the best formulations since smaller pore sizes are beneficial to smoother electrodeposition; this feature makes them a preferable choice for batteries designed for extended cycle life [35,36].

Table 2
Porosity (ε) values of the different membranes.

Samples	ε [%]
3Control	96.4 ± 3.4[a]
3CHI20	97.3 ± 0.5[a]
3CHI40	96.7 ± 0.3[a]
7Control	91.3 ± 1.7[b]
7CHI20	93.1 ± 0.4[b]
7CHI40	92.4 ± 0.3[b]

[a-b] Two means followed by the same letter in the same column are not significantly ($P > 0.05$) different through the Tukey's multiple range test.

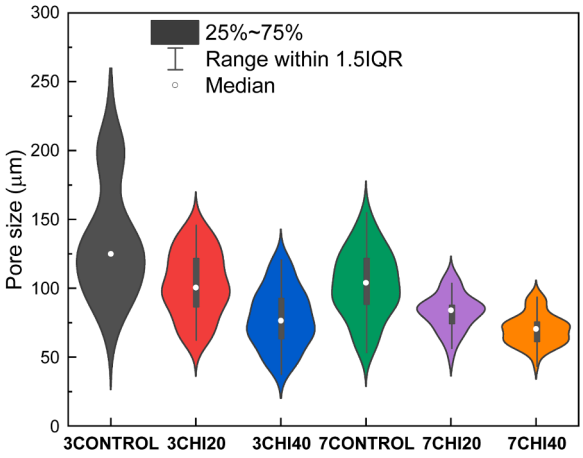


Fig. 2. Pore size for collagen-chitosan membranes.

3.2. Physicochemical characterization

The physicochemical characterization of membranes has been evaluated once suitable thermal and mechanical stability are essential for

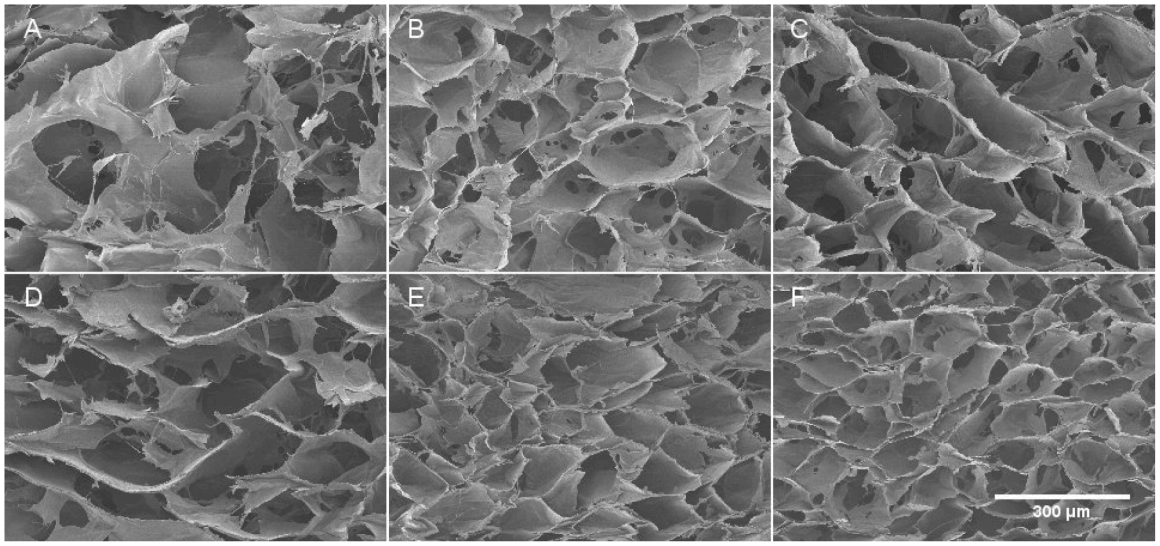


Fig. 1. SEM images from the cross-section of A) 3Control, B) 3CHI20, C) 3CHI40, D) 7Control, E) 7CHI20 and F) 7CHI40 samples.

their use as battery separators [8]. In order to study the interactions among the macromolecules as well as the thermal behavior of collagen-chitosan membranes, FTIR and DSC analyses of 3Control, 3CHI20 and 3CHI40 were performed since it was observed that the polymer concentration in solution did not significantly affect the results of these measurements, as shown in Fig. 3. Concerning FTIR (Fig. 3a)), all samples show the characteristic collagen bands which are related to *C = O* stretching at 1633 cm^{-1} (amide I), N–H bending at 1547 cm^{-1} (amide II) and C–N stretching at 1239 cm^{-1} (amide III) [37,38]. Furthermore, alterations in the relative intensity of amide I and amide II bands were evident upon the addition of chitosan, particularly in samples containing 40 wt % chitosan. These changes in FTIR band intensities strongly indicate the presence of hydrogen bonding interactions among carboxyl, amino, and hydroxyl groups within the membrane components. Further variations observed in the spectral range from 1200 to 900 cm^{-1} are associated with C—O-C and C—O stretching in chitosan, specifically at 1153, 1066, and 1028 cm^{-1} [39].

The effect of collagen-chitosan interactions as a function of collagen content in the thermal properties of the 3Control, 3CHI20 and 3CHI40 samples was assessed by DSC analysis and the results are shown in Fig. 3b). 3Control samples showed two endothermic peaks. The peak around 100 °C is related to the free and bound water release and the peak at around 200 °C corresponded to the collagen denaturation. At the denaturation temperature, the triple-helix structure of collagen turns into gelatin [40,41]. This band changes to a boarder one and its maximum increases to 245 °C with the addition of chitosan [42]. This increase in the denaturation temperature confirmed the presence of physical interactions among collagen and chitosan [39,43]. These results indicate that chitosan containing collagen membranes exhibit adequate thermal stability for potential use as battery separators [44,45].

The changes described above require information about the structure of the samples, as can be provided by XRD analysis (Fig. 3c)). Typically, collagen molecules are organized into fibrils, further aggregating into collagen fibers through intermolecular cross-linking, resulting in the distinctive hierarchical interwoven structure of collagen. This helical arrangement related to the crystalline part of collagen is reflected in the peak at around 7° [46]. According to XRD results, the inclusion of chitosan did not induce significant alterations, confirming the preservation of the collagen helical structure after chitosan incorporation. Additionally, a broad band at around 20° is related to the diffuse scattering of collagen fibers, indicating the amorphous nature of the samples [47], and the third one around 32° is ascribed to the helical rise per residue distance, which is related to the conformational integrity of collagen [46,48]. Therefore, all samples exhibited similar XRD patterns, indicating that the structural integrity of collagen was retained after chitosan addition.

A battery separator must be easy to handle and mechanically stable during the fabrication and operation of the battery. Indeed, a high puncture strength (> 3 N) ensures that both electrodes are kept electrically isolated during cell-assembly and protects against dendritic penetration [49,50]. To assess this, a puncture test was conducted, and the results are presented in Fig. 3d). The maximum force required for the 3Control and 7Control samples were 2.97 ± 0.10 N and 5.12 ± 0.47 N, respectively; these values increased with the addition of chitosan up to 7.33 ± 0.23 N and 8.87 ± 0.59 N for 3CHI40 and 7CHI40 samples,

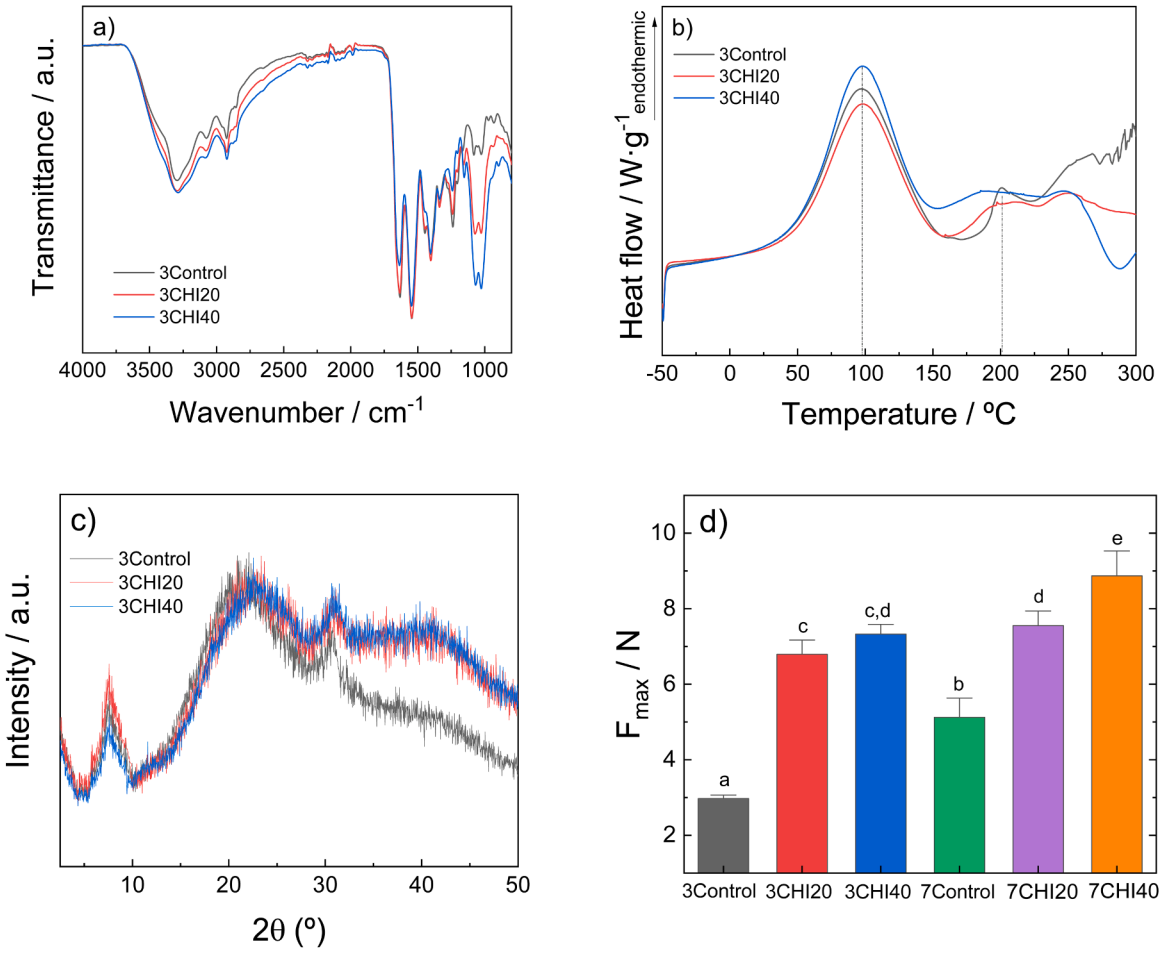


Fig. 3. a) DSC thermograms, b) FTIR spectra, c) XRD patterns, and d) mechanical properties (puncture strength) of collagen-chitosan membranes. [a-e] Two means followed by the same letter in the same column are not significantly ($P > 0.05$) different through the Tukey's multiple range test.

respectively. It is evident that the inclusion of chitosan enhances the mechanical properties of the membranes, which can be related to the physical interactions observed by FTIR analysis, leading to suitable characteristics for their use as lithium-ion battery separators.

3.3. Electrolyte uptake, ionic conductivity, and Li+ transference number

Battery separators should be rapidly swollen when soaked with electrolyte and they should retain the absorbed electrolyte under operating conditions [51]. When the separator ability to interact with the electrolyte is limited, the pores in the separator remain partially unfilled with the liquid electrolyte. As a consequence, this leads to increased electrical resistance due to obstructed pathways for the transportation of Li^+ ions [52]. For this reason, the electrolyte uptake capacity of the membranes as a function of time was measured and the results are presented in Fig. 4a). All the samples showed a fast electrolyte uptake and the membranes reached saturation after 2 h. It can also be observed that the 3Control sample exhibited the highest electrolyte uptake (1150 %) . This value decreased as the polymer concentration in solution and chitosan content increased, obtaining the lowest electrolyte uptake (ELU) values of around 400 wt % for the 7CHI20 and 7CHI40 membranes. The increase in the polymer concentration in solution caused a decrease in the porosity of the membranes, reducing the free volume to be filled by the electrolyte [53]. Further, the physical interactions observed between collagen and chitosan, as identified through FTIR and DSC analyses, affect the arrangement of molecules within the membrane, altering its pore-size distribution and, consequently, the absorption capacity for electrolyte solutions [54]. In any case, all membranes exhibited superior electrolyte absorption capacity, surpassing that of cellulose paper (195 %) and significantly outperforming PP membranes (91 %) [55]. This is attributed to the fact of chitosan and collagen having abundant polar functional groups (-COOH, $-NH_2$ and –OH), with affinity to polar organic solvents [56]. It must also be mentioned that these biopolymers exhibit excellent stability in polar electrolytes due to their chemical structure [57].

Following the absorption process, the ionic conductivity was assessed using impedance spectroscopy, and the Nyquist plot for all membranes are depicted in Fig. 4b). The Nyquist plot exhibits a straight line across the frequency range, indicating the high ionic conduction process involving charge transfer and the Li electrode/electrolyte interface for all membranes [58]. These results reveal a complex interaction between the composition of the membranes and their electrolyte absorption capacity, influencing ionic conductivity in the system. It can be observed that the increased electrolyte absorption does not necessarily translate into higher ionic conductivity. The ionic conductivity was calculated from Eq. (3), where the resistance value obtained from the equivalent circuit and the respective values are shown in Table 3. For the membranes with lower collagen content, the addition of chitosan positively influences ionic conductivity, but can also lead to complex interactions. Both chitosan and collagen have, which the positive charge can interact with the oppositely charged entities in the liquid electrolyte and these interactions can influence the ionic conductivity of the membrane [59]. Nevertheless, it can be concluded that both 3CHI20 and 3CHI40 exhibit the lowest resistance and consequently high ionic conductivity value, i.e., 0.71 and 0.90 $mS{\cdot}cm^{-1}$. For the membranes with higher polymer content, the addition of chitosan does not significantly

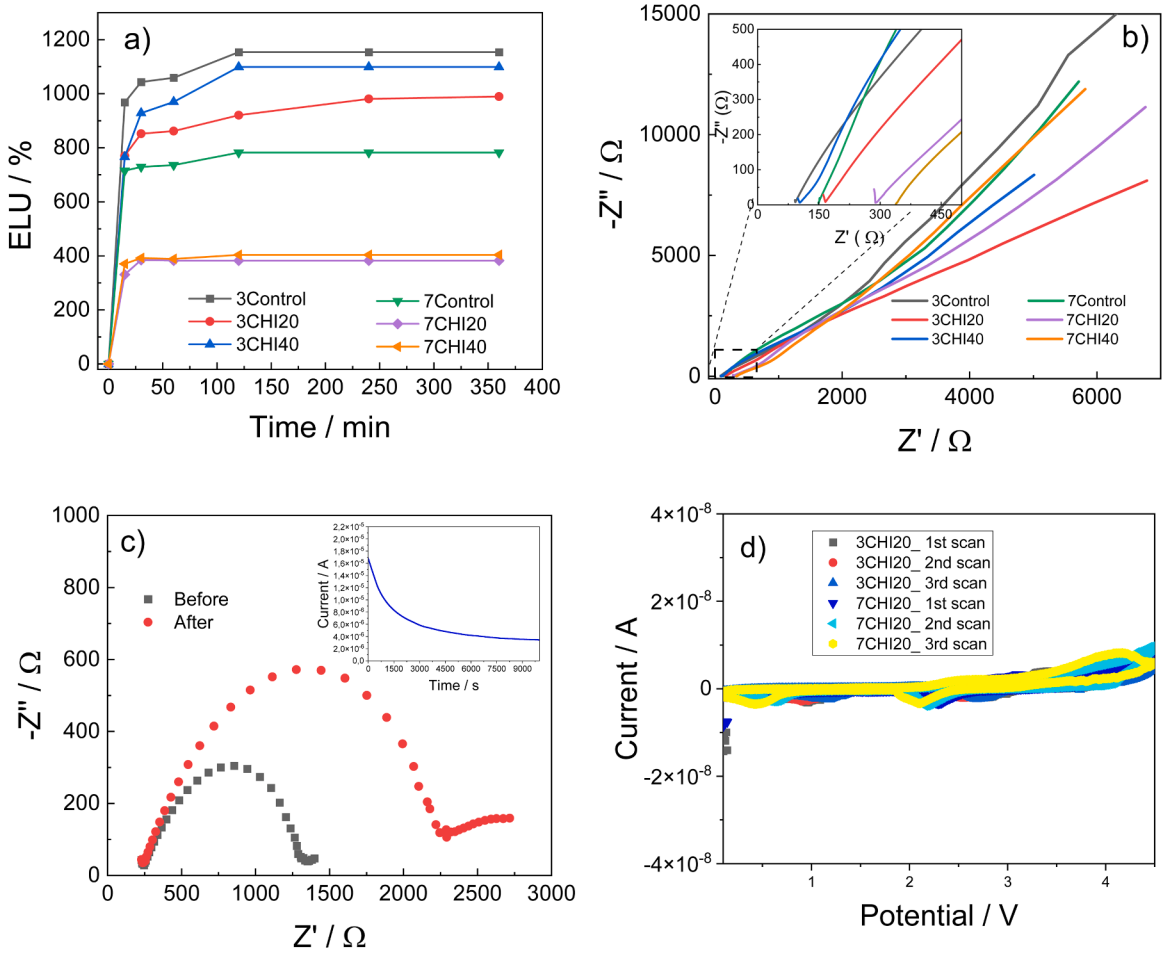


Fig. 4. a) Electrolyte uptake as a function of time, b) Nyquist plot, c) DC polarization measurements and current as a function of time (inset) for 7CHI20 sample and d) Cyclic voltammogram of the 3CHI20 and 7CHI20 samples.

Table 3
Ionic conductivity (σ_i), and lithium transference number values of the collagen-chitosan membranes at room temperature.

Samples	σ_i (mS·cm^{-1} ± 0.3)	t_{Li+}
3Control	0.90	0.20
3CHI20	0.71	0.20
3CHI40	0.90	0.20
7Control	1.58	0.20
7CHI20	0.54	0.20
7CHI40	0.49	0.20

improve ionic conductivity, possibly due to a higher polymer network density that restrict ionic mobility. In any case, the ionic conductivity values of all the samples were similar, ranging between 0.49 and 1.58 mS·cm^{-1}. The lithium transference values for all samples was also obtained by chronoamperometry measurements and the results are shown in Table 3. For this measurement, the Bruce and Evans method was used [60], and the value obtained is 0.2, regardless of the chitosan and samples porosity. Additionally, Fig. 4c) showing the chronoamperometry measurements for the 7CHI20 sample.

The electrochemical stability of the separator samples was assessed using cyclic voltammetry, as illustrated in Fig. 4d It is shown that no notable peaks that could impact battery performance are observed, the current value being very low.

3.4. Charge/discharge battery behavior

Cathodic half-cells with the collagen-chitosan membranes as separators were assembled in order to assess the battery performance at different C-rates (C/8–2C) from 2.5 to 4.2 V at room temperature. Ten charge–discharge cycles were performed at each C-rate and the fifth charge/discharge curve profiles at C/8, C/5, C/2, and 1C-rate for the 7CHI20 membrane are depicted in Fig. 5a). The charge/discharge cycles reveal a remarkably consistent curve profile throughout the cycle sequence. Fig. 5a) exhibits the distinctive cathodic/anodic peaks characteristic of C-LFP active materials, delineating lithium removal during charging and lithium insertion during discharge. With an increase in C-rate, a decrease in capacity is evident, attributed to Ohmic polarization [61]. The obtained discharge capacity values are 164, 154, 133 and 58 mAh·g^{-1} for C/8, C/5, C/2, and 1C rates, respectively.

To compare the charge/discharge profiles between the membranes, Fig. 5b) illustrates the corresponding profile curves at the C/5-rate. The discharge capacities for the different membranes are as follows: 140, 135, 124, 137, 164, and 135 mAh·g^{-1} for the 3Control, 3CHI20, 3CHI40, 7Control, 7CHI20, and 7CHI40 membranes, respectively. It is evident that the 7CHI20 membrane exhibits the highest discharge capacities among the tested membranes at the C/5-rate. Fig. 5c) shows the rate performance of all membranes, depicting the discharge capacity as a function of cycle number. All membranes showed good cycling stability throughout the cycle number and the discharge capacity value is higher

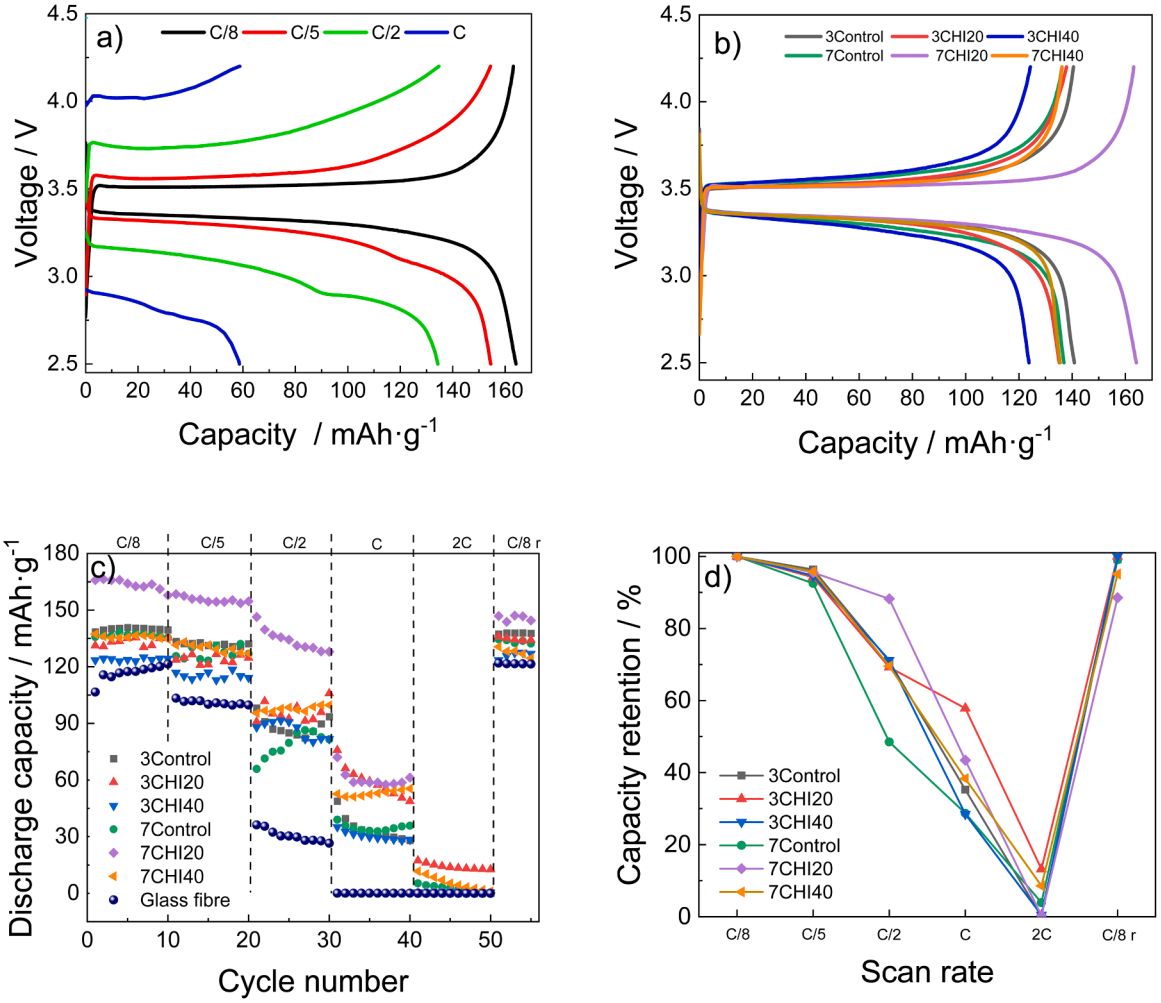


Fig. 5. a) Representative charge/discharge profiles for the cathodic half-cells for the (7CHI20 membranes), b) first charge/discharge profile at C/5-rate for cathodic cells prepared with both collagen and collagen-chitosan membranes, c) rate performance with the different collagen, collagen-chitosan and glass fibre separators, and d) capacity retention for the half-cell batteries.

when compared to commercial glass fibre separator, indicating excellent interaction between the electrolyte solution with chitosan and collagen polymer. It is observed that the 7CHI20 membrane, exhibited the most favorable discharge capacity values, showing an outstanding battery behavior. Furthermore, a close correspondence is noted between the discharge and charge values for all C-rates, suggesting minimal charge loss during the process and so, indicating a coulombic efficiency close to 100 % [62]. Indeed, the electrochemical stability and efficiency in capturing and releasing electrical charge in the 3CHI20 membranes can be emphasized at high C rates. Additionally, the consistent results across different charging rates highlight the reproducibility and stability of the system.

Additionally, Fig. 5d) presents the capacity retention for membranes during the discharge process normalized to the C/8 rate. Regardless of membrane composition, a decrease in capacity retention is observed due to the lithium diffusion phenomenon between the separator membrane and cathode electrode [63]. Moreover, all membranes exhibit an excellent reversibility process, as the discharge capacity at C/8, after the C-rate test, returns to its initial value in all samples.

Considering that 3CHI20 membranes exhibit excellent cycling behavior at high C-rates, Fig. 6a) shows the charge and discharge value for this sample at C and 2C-rates over 100 cycles. It is observed that coulombic efficiency is very close to 100 %, with a discharge capacity value at C-rate of 52 and 42 $mAh{\cdot}g^{-1}$ for the first and 100 cycle respectively, the capacity fade being around 20 %. Also, it is detected that, after >200 cycles, this sample presents an excellent recovery capacity value (Fig. 6a).

To enhance our understanding of the battery performance exhibited by the collagen-chitosan membranes, Electrochemical Impedance Spectroscopy (EIS) was performed both prior to and after galvanostatic cycling, as illustrated in Fig. 6b, where the Nyquist plot of the cathodic half-cells featuring the 3CHI20 membrane is presented before and after cycling. In both Nyquist plots, a semicircle is discernible at high-frequency range, along with a straight line at the lower-frequency range. The semicircle characterizes the interfacial and charge transfer resistances, while the straight line delineates the Li^+ diffusion process, i.e., the membrane/electrode interface [64]. Notably, cycling induces an increase in resistance from 880 Ω to 1632 Ω, attributed to the formation of the solid electrolyte interphase (SEI) layer during cycling. The formation of a SEI is a complex process occurring in lithium-ion batteries during initial charge and discharge cycles. As the lithium ions move from the cathode to the anode during the first charge, interactions between the electrolyte components and the anode lead to the creation of secondary products. These secondary products undergo electrochemical reactions with lithium in the anode, resulting in the development of a thin layer of solid compounds known as the SEI. The SEI serves as a crucial protective role, acting as a barrier that prevents direct reactions between the liquid electrolyte and the lithium metal in the anode, thereby mitigating issues such as lithium dendrite formation and improving battery safety and longevity. Over time, the SEI continues to evolve and stabilizes through subsequent charge-discharge cycles, influencing the overall performance and aging characteristics of the battery [65].

Table 4 compares the ionic conductivity value and discharge capacity value of the sustainable separator developed in this work with other separators based on sustainable polymers reported in the literature.

This is the first time that this collagen and chitosan-based porous membrane has been reported as a separator for lithium-ion battery applications, in which its battery performance is comparable to other sustainable separators.

In summary, this work demonstrates that it is possible to produce battery separator membranes based on collagen and chitosan with excellent cycling performance. The best membrane with high values of discharge capacity at high C rates was the 3CHI20 sample. This highlights the potential of sustainable separators created through this method.

3.5. Environmental assessment

In the manufacturing stage of separators for lithium-ion batteries, the freeze-drying process exhibited the highest environmental impact throughout the life cycle of collagen-chitosan membranes (Fig. 7). Freeze-drying emerged as the primary contributor to the overall environmental burden across all impact categories. Specifically, freeze-drying had a significant influence on categories such as global warming, terrestrial acidification, and marine eutrophication, with its contribution exceeding 93 % in most cases.

When comparing our results with a previous study that analyzed the environmental impact of collagen and chitosan scaffolds [27], we observed several key differences. The previous study used glycerol as a plasticizer and mechanical stirring in its process. The results of that study showed that the marine eutrophication and land use categories were significantly influenced by the use of glycerol, with contributions of 20 % and 17.5 % respectively. Furthermore, mechanical stirring significantly impacted the analyzed categories, with contributions ranging from 29 % to 48 %. In contrast, our study did not use glycerol and significantly reduced the impact of mechanical stirring by using Ultraturrax, which accounted for only 2.5 % to 6 % of the impact in the analyzed categories. In the previous study, freeze-drying was also a significant contributor to the environmental impact, but its impact was more evenly distributed with other processes, such as the use of glycerol

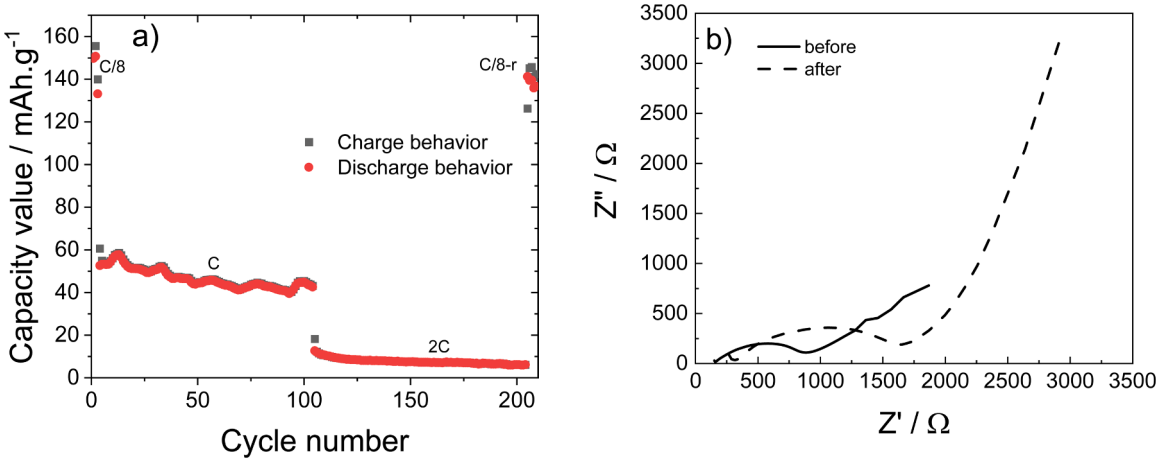


Fig. 6. a) Cycle life at C and 2C rate for 100 cycles and b) Nyquist plot before and after galvanostatic cycling for the 3CHI20 membrane.

Table 4
Sustainable separator membranes applied in LIB applications.

Polymer matrix	Electrolyte	Porosity/ Uptake (%)	Ionic condutivity ($mS.cm^{-1}$)	Discharge capacity ($mAh.g^{-1}$)	Ref
Mesoporous cellulose nanocrystal (MCNC)	1 M LiPF6 in EC:DMC and ionic liquid, 1-ethyl-3-methylimidazolium bis(trifluoromethylsulfonyl)imide, [C2 mim][NTf2]	75.3/275	2.7	85@2C	[66]
Poly(L-lactic acid), PLLA	1 M LiPF6 in EC:DMC	72.7/350	1.6	93@C	[67]
Silk fibroin	1 M LiPF6 in EC:DMC	65/1100	0.32	54@2C	[68]
Silk fibroin/sericin	1 M LiPF6 in EC:DMC	85/160	4.09	85@2C	[69]
Poly(3-Hydroxybutyrate-Co-Hydroxyvalerate), PHBV	1 M LiPF6 in EC:DMC	—/300	5.2	30@C	[70]
Carrageenan	1 M LiPF6 in EC:DMC	90/700	1.34	25@C	[71]
Cellulose/soy	1 M LiPF6 in EC:DMC	85/>1000	5.8	112@C	[72]
Wool/soy	1 M LiPF6 in EC:DMC	83/400	1.22	40@2C	[73]
Collagen/Chitosan	1 M LiPF6 in EC:DMC	97.3/~900	0.71	42@C	In this work

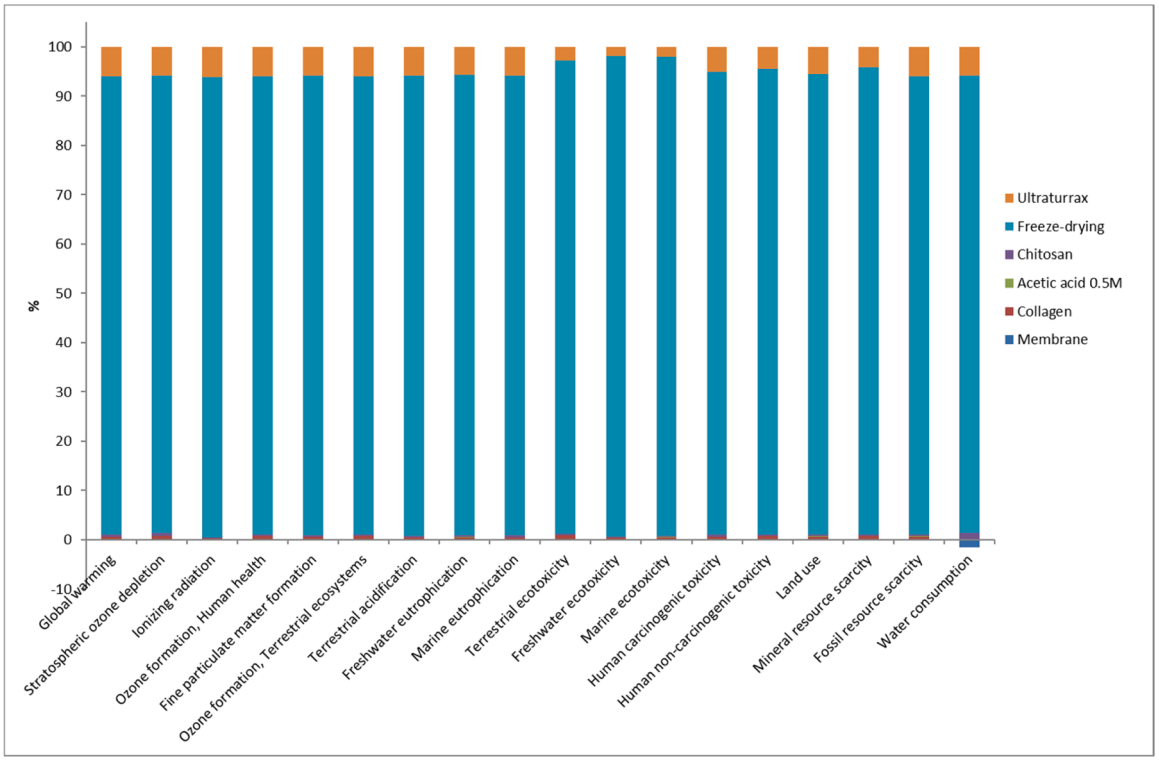


Fig. 7. Relative contributions in each impact category for the most relevant processes involved in the manufacture of collagen-chitosan samples.

and mechanical stirring. Therefore, it is worth noting that the absence of glycerol and the replacement of mechanical stirring by mixing with Ultraturrax are proved environmentally friendlier options to manufacture the membranes. However, addressing the impact of freeze-drying and exploring improvements in the process could be a crucial advance towards more sustainable production practices. In this regard, freeze-drying process could be optimized by reducing energy consumption through the implementation of more energy-efficient freeze-drying technologies, such as optimized cycles that minimize processing time [74]. Additionally, integrating renewable energy sources, such as solar panels or wind energy, to power the freeze-drying process could help reducing greenhouse gas emissions. Finally, with industrial scaling, freeze-drying could lead to a relatively lower impact, as larger quantities of membranes could be processed in a single cycle. This would increase process efficiency and reduce environmental impact. Additionally, other manufacture processes could be explored to develop porous membranes. In particular, electrospinning, a process that uses an electric field to produce fine fibers from a polymeric solution, could offer advantages in terms of energy consumption reduction, resulting in porous structures suitable for lithium-ion battery separators.

4. Conclusions

Considering the circular economy and sustainability issues for the development of added value products through the valorization of waste materials, in this work sustainable membranes, based on collagen and chitosan with different amounts of each polymer, were prepared by freeze-drying. Regardless of the membrane composition, a porous morphology with interconnected pores and porosity above 90 % is obtained, where the pore size is affected by the polymer concentration. For all membranes, a high electrolyte uptake process above 400 % is obtained. The use of chitosan increases mechanical and thermal stability compared to pure collagen-based membranes. According to the electrochemical results, the collagen content has the largest impact on the ionic conductivity value, which is greater than 0.49 mS·cm-1 for all membranes. Furthermore, these membranes allow battery cycling at room temperature for various C rates and show discharge capabilities larger than 140 mAh·g-1 at C/8 rate. The lithium transference number of

these membranes is 0.20. The best membrane for C and 2C rates is 3CHI20 due to its ionic conductivity value and presents 42 mAh·g-1 after 100 cycles at C rate, indicating excellent reversibility process. In addition to the battery performance, the environmental assessment associated to the development of the membranes revealed that the freeze-drying process is the most significant contributor in relation to all the stages involved in the production of the membranes. Therefore, reducing energy consumption through the optimization of this process and the integration of renewable energy sources is proposed as an improvement towards more sustainable manufacture processes. Given the demand to combine more environmentally friendly materials and advanced applications aligned with the circular economy paradigm, the membranes developed in this study offer a promising replacement for conventional LIB separators.

CRediT authorship contribution statement

Mireia Andonegi: Writing – review & editing, Writing – original draft, Visualization, Methodology, Investigation, Data curation, Conceptualization, Formal analysis. **João P. Serra:** Writing – original draft, Formal analysis, Investigation, Methodology. **Maria M. Silva:** Resources, Writing – review & editing. **Renato Gonçalves:** Resources, Validation, Visualization, Writing – review & editing. **Carlos M. Costa:** Writing – review & editing, Validation, Supervision, Resources, Project administration, Methodology, Funding acquisition, Formal analysis, Conceptualization. **Senentxu Lanceros-Mendez:** Writing – review & editing, Validation, Supervision, Resources, Project administration, Funding acquisition, Conceptualization. **Koro de la Caba:** Writing – review & editing, Validation, Resources, Project administration, Funding acquisition. **Pedro Guerrero:** Writing – review & editing, Data curation, Validation, Supervision, Methodology.

Declaration of competing interest

The authors declare that they have no known competing financial interests or personal relationships that could have appeared to influence the work reported in this paper.

Acknowledgements

This work was supported by the Fundação para a Ciência e Tecnologia (FCT) under the framework of Strategic Funding UIDB/04650/2020, UID/FIS/04650/2020, UID/EEA/04436/2020, and UID/QUI/00686/2020, and under projects POCI-01–0247-FEDER-046985 and 10.54499/2022.03931.PTDC, funded by national funds through FCT and by the ERDF through the COMPETE2020—Programa Operacional Competitividade e Internacionalização (POCI). NGS-New Generation Storage, C644936001–00000045, was supported by IAPMEI (Portugal) with funding from the European Union NextGenerationEU (PRR). This work was supported by the Fundação para a Ciência e Tecnologia (FCT) under Grant 10.54499/2021.08158.BD (J.P.S.) and FCT investigator contracts CEECIND/00833/2017 (R.G) and 2020.04028.CEECIND (C.M.C.). This study forms part of the Advanced Materials program and was supported by MCIN with funding from the European Union NextGenerationEU (PRTR-C17.I1) and by the Basque Government under the IKUR program. This work was also supported by the Basque Government (IT1658–22 and POS_2022_1_0007) and PID2021–124294OB-C22 funded by MCI/AEI and by "ERDF A way of making Europe". The authors thank for technical and human support provided by SGIker (UPV/EHU/ERDF, EU).

References

[1] R.E. Smalley, Future global energy prosperity: the terawatt challenge, MRS Bull. 30 (6) (2005) 412–417, https://doi.org/10.1557/mrs2005.124.
[2] P.J. Hall, Energy storage: the route to liberation from the fossil fuel economy? Energy Pol. 36 (12) (2008) 4363–4367, https://doi.org/10.1016/j.enpol.2008.09.041.
[3] U. Datta, A. Kalam, J. Shi, A review of key functionalities of battery energy storage system in renewable energy integrated power systems, Energy Storage 3 (5) (2021) e224, https://doi.org/10.1002/est2.224.
[4] Y. Sun, Z. Zhao, M. Yang, D. Jia, W. Pei, B. Xu, Overview of energy storage in renewable energy power fluctuation mitigation, CSEE J. Power Energy Syst. 6 (1) (2020) 160–173, https://doi.org/10.17775/CSEEJPES.2019.01950.
[5] M. Zschornak, F. Meutzner, J. Lück, A. Latz, T. Leisegang, J. Hanzig, M. Nentwich, J. Zosel, P.B. Balbuena, Fundamental principles of battery design 3 (11) (2018), https://doi.org/10.1515/psr-2017-0111.
[6] M. Alizadeh, F. Abbasi, A.B. Khoshfetrat, H. Ghaleh, Microstructure and characteristic properties of gelatin/chitosan scaffold prepared by a combined freeze-drying/leaching method, Mater Sci. Eng. C Mater. Biol. Appl. 33 (7) (2013) 3958–3967, https://doi.org/10.1016/j.msec.2013.05.039.
[7] M. Li, J. Lu, Z. Chen, K. Amine, 30 Years of lithium-ion batteries, Adv. Mater. 30 (33) (2018) 1800561, https://doi.org/10.1002/adma.201800561.
[8] C.M. Costa, E. Lizundia, S. Lanceros-Méndez, Polymers for advanced lithium-ion batteries: state of the art and future needs on polymers for the different battery components, Prog. Energy Combust. Sci. 79 (2020) 100846, https://doi.org/10.1016/j.pecs.2020.100846.
[9] A. Manthiram, An outlook on lithium ion battery technology, ACS Cent. Sci. 3 (10) (2017) 1063–1069, https://doi.org/10.1021/acscentsci.7b00288.
[10] A.G. Olabi, Q. Abbas, P.A. Shinde, M.A. Abdelkareem, Rechargeable batteries: technological advancement, challenges, current and emerging applications, Energy 266 (2023) 126408, https://doi.org/10.1016/j.energy.2022.126408.
[11] K.K. Jana, S.J. Lue, A. Huang, J.F. Soesanto, K.-L. Tung, Separator membranes for high energy-density batteries, ChemBioEng Rev. 5 (6) (2018) 346–371, https://doi.org/10.1002/cben.201800014.
[12] P. Zhai, K. Liu, Z. Wang, L. Shi, S. Yuan, Multifunctional separators for high-performance lithium ion batteries, J. Power Sources 499 (2021) 229973, https://doi.org/10.1016/j.jpowsour.2021.229973.
[13] M. Waqas, S. Ali, C. Feng, D. Chen, J. Han, W. He, Recent development in separators for high-temperature lithium-ion batteries, Small. 15 (33) (2019) 1901689, https://doi.org/10.1002/smll.201901689.
[14] P. Arora, Z. Zhang, Battery Separators, Chem. Rev. 104 (10) (2004) 4419–4462, https://doi.org/10.1021/cr020738u.
[15] W. Zhang, Z. Tu, J. Qian, S. Choudhury, L.A. Archer, Y. Lu, Design principles of functional polymer separators for high-energy, metal-based batteries, Small 14 (11) (2018) 1703001, https://doi.org/10.1002/smll.201703001.
[16] L. Li, Y. Duan, Engineering polymer-based porous membrane for sustainable lithium-ion battery separators, Polymers (2023).
[17] C. Maraveas, Production of sustainable and biodegradable polymers from agricultural waste, Polymers (2020).
[18] E. Lizundia, C.M. Costa, R. Alves, S. Lanceros-Méndez, Cellulose and its derivatives for lithium ion battery separators: a review on the processing methods and properties, Carbohydrate Polymer Technol. Appl. 1 (2020) 100001, https://doi.org/10.1016/j.carpta.2020.100001.
[19] M. Andonegi, D.M. Correia, N. Pereira, C.M. Costa, S. Lanceros-Mendez, K. de la Caba, P. Guerrero, Sustainable collagen composites with graphene oxide for bending resistive sensing, Polymers (2023).
[20] P. Fratzl, K. Misof, I. Zizak, G. Rapp, H. Amenitsch, S. Bernstorff, Fibrillar structure and mechanical properties of collagen, J. Struct. Biol. 122 (1) (1998) 119–122, https://doi.org/10.1006/jsbi.1998.3966.
[21] X. Zhang, S. Xu, L. Shen, G. Li, Factors affecting thermal stability of collagen from the aspects of extraction, processing and modification, Journal of Leather Science and Engineering 2 (1) (2020) 19, https://doi.org/10.1186/s42825-020-00033-0.
[22] S. Kou, L.M. Peters, M.R. Mucalo, Chitosan: a review of sources and preparation methods, Int. J. Biol. Macromol. 169 (2021) 85–94, https://doi.org/10.1016/j.ijbiomac.2020.12.005.
[23] A. Irastorza, I. Zarandona, M. Andonegi, P. Guerrero, K. de la Caba, The versatility of collagen and chitosan: from food to biomedical applications, Food Hydrocoll. 116 (2021) 106633, https://doi.org/10.1016/j.foodhyd.2021.106633.
[24] V. Vijayakumar, S.Y. Nam, A review of recent Chitosan Anion exchange membranes for polymer electrolyte membrane fuel cells, Membranes (2022).
[25] Y. Song, G. Zhao, S. Zhang, C. Xie, R. Yang, X. Li, Chitosan nanofiber paper used as separator for high performance and sustainable lithium-ion batteries, Carbohydr. Polym. (2023) 121530, https://doi.org/10.1016/j.carbpol.2023.121530.
[26] R. Gonçalves, P. Dias, L. Hilliou, P. Costa, M.M. Silva, C.M. Costa, S. Corona-Galván, S. Lanceros-Méndez, Optimized printed cathode electrodes for high performance batteries, Energy Technol. 9 (1) (2021) 2000805, https://doi.org/10.1002/ente.202000805.
[27] M. Andonegi, A. Irastorza, A. Izeta, S. Cabezudo, K. de la Caba, P. Guerrero, A green approach towards native collagen scaffolds: environmental and physicochemical assessment, Polymers (2020).
[28] I. Leceta, P. Guerrero, S. Cabezudo, K.d.l. Caba, Environmental assessment of chitosan-based films, J. Clean Prod. 41 (2013) 312–318, https://doi.org/10.1016/j.jclepro.2012.09.049.
[29] Z. Fereshteh, 7 - Freeze-drying technologies for 3D scaffold engineering, in: Y. Deng, J. Kuiper (Eds.), Functional 3D Tissue Engineering Scaffolds, Woodhead Publishing, 2018, pp. 151–174, https://doi.org/10.1016/B978-0-08-100979-6.00007-0.
[30] K. Lin, D. Zhang, M.H. Macedo, W. Cui, B. Sarmento, G. Shen, Advanced collagen-based biomaterials for regenerative biomedicine, Adv. Funct Mater. 29 (3) (2019) 1804943, https://doi.org/10.1002/adfm.201804943.

[31] A. Dewle, N. Pathak, P. Rakshasmare, A. Srivastava, Multifarious fabrication approaches of producing aligned collagen scaffolds for tissue engineering applications, ACS Biomater. Sci. Eng. 6 (2) (2020) 779–797, https://doi.org/10.1021/acsbiomaterials.9b01225.
[32] C. Katrilaka, N. Karipidou, N. Petrou, C. Manglaris, G. Katrilakas, A.N. Tzavellas, M. Pitou, E.E. Tsiridis, T. Choli-Papadopoulou, A. Aggeli, Freeze-drying process for the fabrication of collagen-based sponges as medical devices in biomedical engineering, Materials (2023).
[33] D.E.L. Angulo, P.J.d.A. Sobral, The effect of processing parameters and solid concentration on the microstructure and pore architecture of gelatin-chitosan scaffolds produced by freeze-drying, Mater. Res. 19 (2016) 839–845.
[34] S. Yan, X. Chen, P. Zhou, P. Wang, H. Zhou, W. Zhang, Y. Xia, K. Liu, Regulating the growth of lithium dendrite by coating an ultra-thin layer of gold on separator for improving the fast-charging ability of graphite anode, J. Energy Chem. 67 (2022) 467–473, https://doi.org/10.1016/j.jechem.2021.10.036.
[35] D. Miranda, R. Gonçalves, S. Wuttke, C.M. Costa, S. Lanceros-Méndez, Overview on theoretical simulations of lithium-ion batteries and their application to battery separators, Adv. Energy Mater. 13 (13) (2023) 2203874, https://doi.org/10.1002/aenm.202203874.
[36] W. Luo, S. Cheng, M. Wu, X. Zhang, D. Yang, X. Rui, A review of advanced separators for rechargeable batteries, J. Power Sources 509 (2021) 230372, https://doi.org/10.1016/j.jpowsour.2021.230372.
[37] T. Riaz, R. Zeeshan, F. Zarif, K. Ilyas, N. Muhammad, S.Z. Safi, A. Rahim, S.A. A. Rizvi, I.U. Rehman, FTIR analysis of natural and synthetic collagen, Appl. Spectrosc. Rev. 53 (9) (2018) 703–746, https://doi.org/10.1080/05704928.2018.1426595.
[38] S. Noorzai, C.J.R. Verbeek, M.C. Lay, J. Swan, Collagen extraction from various waste bovine hide sources, Waste BioMass Valorizat. 11 (11) (2020) 5687–5698, https://doi.org/10.1007/s12649-019-00843-2.
[39] M. Andonegi, K.L. Heras, E. Santos-Vizcaíno, M. Igartua, R.M. Hernandez, K. de la Caba, P. Guerrero, Structure-properties relationship of chitosan/collagen films with potential for biomedical applications, Carbohydr. Polym. 237 (2020) 116159, https://doi.org/10.1016/j.carbpol.2020.116159.
[40] D. Derman İ, E.C. Şenel, O. Ferhanoğlu, İ. Çilesiz, M. Kazanci, Effect of heat level and expose time on denaturation of collagen tissues, Cell. Mol. Bioeng. 14 (1) (2021) 113–119, https://doi.org/10.1007/s12195-020-00653-w.
[41] S. El Moujahed, F. Errachidi, H. Abou Oualid, A.-V. Botezatu-Dediu, F. Ouazzani Chahdi, Y. Kandri Rodi, R.M. Dinica, Extraction of insoluble fibrous collagen for characterization and crosslinking with phenolic compounds from pomegranate byproducts for leather tanning applications, RSC Adv 12 (7) (2022) 4175–4186, https://doi.org/10.1039/D1RA08059H.
[42] Z. Osman, Thermal and conductivity studies of chitosan acetate-based polymer electrolytes, Ionics (Kiel) 11 (5) (2005) 397–401, https://doi.org/10.1007/BF02430254.
[43] C.C. Silva, C.G.A. Lima, A.G. Pinheiro, J.C. Góes, S.D. Figueiró, A.S.B. Sombra, On the piezoelectricity of collagen–chitosan films, Phys. Chem. Chem. Phys. 3 (18) (2001) 4154–4157, https://doi.org/10.1039/B100189M.
[44] H. Zheng, R. Yang, G. Liu, X. Song, V.S. Battaglia, Cooperation between active material, polymeric binder and conductive carbon additive in lithium ion battery cathode, J. Phys. Chem. C 116 (7) (2012) 4875–4882, https://doi.org/10.1021/jp208428w.
[45] M.H. Parekh, S. Oka, J. Lutkenhaus, V.G. Pol, Critical-point-dried, porous, and safer aramid nanofiber separator for high-performance durable lithium-ion batteries, ACS Appl. Mater. Interfaces 14 (25) (2022) 29176–29187, https://doi.org/10.1021/acsami.2c04630.
[46] Z. Meng, X. Zheng, K. Tang, J. Liu, Z. Ma, Q. Zhao, Dissolution and regeneration of collagen fibers using ionic liquid, Int. J. Biol. Macromol. 51 (4) (2012) 440–448, https://doi.org/10.1016/j.ijbiomac.2012.05.030.
[47] M. Andonegi, T. Carranza, A. Etxabide, K. de la Caba, P. Guerrero, 3D-Printed mucoadhesive collagen scaffolds as a local tetrahydrocurcumin delivery system, Pharmaceutics. (2021).
[48] Y. Hu, L. Liu, W. Dan, N. Dan, Z. Gu, Evaluation of 1-ethyl-3-methylimidazolium acetate based ionic liquid systems as a suitable solvent for collagen, J. Appl. Polym Sci. 130 (4) (2013) 2245–2256, https://doi.org/10.1002/app.39298.
[49] Z. Lu, F. Sui, Y.-E. Miao, G. Liu, C. Li, W. Dong, J. Cui, T. Liu, J. Wu, C. Yang, Polyimide separators for rechargeable batteries, J. Energy Chem. 58 (2021) 170–197, https://doi.org/10.1016/j.jechem.2020.09.043.
[50] H.S. Bierenbaum, R.B. Isaacson, M.L. Druin, S.G. Plovan, Microporous polymeric films, Product R&D 13 (1) (1974) 2–9, https://doi.org/10.1021/i360049a002.
[51] S.S. Zhang, A review on the separators of liquid electrolyte Li-ion batteries, J Power Sources 164 (1) (2007) 351–364, https://doi.org/10.1016/j.jpowsour.2006.10.065.
[52] J.-A. Choi, S.H. Kim, D.-W. Kim, Enhancement of thermal stability and cycling performance in lithium-ion cells through the use of ceramic-coated separators, J. Power Sources 195 (18) (2010) 6192–6196, https://doi.org/10.1016/j.jpowsour.2009.11.020.
[53] P. Raghavan, J. Manuel, X. Zhao, D.-S. Kim, J.-H. Ahn, C. Nah, Preparation and electrochemical characterization of gel polymer electrolyte based on electrospun polyacrylonitrile nonwoven membranes for lithium batteries, J. Power Sources 196 (16) (2011) 6742–6749, https://doi.org/10.1016/j.jpowsour.2010.10.089.
[54] B.S. Kumar, S. Aigal, D.V. Ramesh, Air-dried 3D-collagen–chitosan biocomposite scaffold for tissue engineering application, Polym Compos 33 (11) (2012) 2029–2035, https://doi.org/10.1002/pc.22345.
[55] D. Lv, J. Chai, P. Wang, L. Zhu, C. Liu, S. Nie, B. Li, G. Cui, Pure cellulose lithium-ion battery separator with tunable pore size and improved working stability by cellulose nanofibrils, Carbohydr. Polym. 251 (2021) 116975, https://doi.org/10.1016/j.carbpol.2020.116975.
[56] C. Cheng, R. Yang, Y. Wang, D. Fu, J. Sheng, X. Guo, A bacterial cellulose-based separator with tunable pore size for lithium-ion batteries, Carbohydr. Polym 304 (2023) 120489, https://doi.org/10.1016/j.carbpol.2022.120489.
[57] M.F. Lagadec, R. Zahn, V. Wood, Characterization and performance evaluation of lithium-ion battery separators, Nat. Energy 4 (1) (2019) 16–25, https://doi.org/10.1038/s41560-018-0295-9.
[58] J.C. Barbosa, D.M. Correia, R. Gonçalves, V. de Zea Bermudez, M.M. Silva, S. Lanceros-Mendez, C.M. Costa, Enhanced ionic conductivity in poly(vinylidene fluoride) electrospun separator membranes blended with different ionic liquids for lithium ion batteries, J. Colloid Interface Sci. 582 (2021) 376–386, https://doi.org/10.1016/j.jcis.2020.08.046.
[59] H. Xu, Y. Wang, X. Liao, B. Shi, A collagen-based electrolyte-locked separator enables capacitor to have high safety and ionic conductivity, J. Energy Chem. 47 (2020) 324–332, https://doi.org/10.1016/j.jechem.2020.02.001.
[60] J. Evans, C.A. Vincent, P.G. Bruce, Electrochemical measurement of transference numbers in polymer electrolytes, Polymer 28 (13) (1987) 2324–2328, https://doi.org/10.1016/0032-3861(87)90394-6.
[61] A. Gören, J. Mendes, H.M. Rodrigues, R.E. Sousa, J. Oliveira, L. Hilliou, C.M. Costa, M.M. Silva, S. Lanceros-Méndez, High performance screen-printed electrodes prepared by a green solvent approach for lithium-ion batteries, J. Power Sources 334 (2016) 65–77, https://doi.org/10.1016/j.jpowsour.2016.10.019.
[62] J. Xiao, Q. Li, Y. Bi, M. Cai, B. Dunn, T. Glossmann, J. Liu, T. Osaka, R. Sugiura, B. Wu, J. Yang, J.-G. Zhang, M.S. Whittingham, Understanding and applying coulombic efficiency in lithium metal batteries, Nat. Energy 5 (8) (2020) 561–568, https://doi.org/10.1038/s41560-020-0648-z.
[63] S.H. Lee, J. Kim, B.-H. Kim, S. Yoon, K.Y. Cho, Delamination-free multifunctional separator for long-term stability of lithium-ion batteries, Small. 15 (12) (2019) 1804980, https://doi.org/10.1002/smll.201804980.
[64] C.M. Costa, V. Sencadas, J.G. Rocha, M.M. Silva, S. Lanceros-Méndez, Evaluation of the main processing parameters influencing the performance of poly(vinylidene fluoride–trifluoroethylene) lithium-ion battery separators, J. Solid State Electrochem. 17 (3) (2013) 861–870, https://doi.org/10.1007/s10008-012-1928-8.
[65] S.J. An, J. Li, C. Daniel, D. Mohanty, S. Nagpure, D.L. Wood, The state of understanding of the lithium-ion-battery graphite solid electrolyte interphase (SEI) and its relationship to formation cycling, Carbon N Y 105 (2016) 52–76, https://doi.org/10.1016/j.carbon.2016.04.008.
[66] R. Gonçalves, E. Lizundia, M.M. Silva, C.M. Costa, S. Lanceros-Méndez, Mesoporous cellulose nanocrystal membranes as battery separators for environmentally safer lithium-ion batteries, ACS. Appl. Energy Mater. 2 (5) (2019) 3749–3761, https://doi.org/10.1021/acsaem.9b00458.
[67] J.C. Barbosa, A. Reizabal, D.M. Correia, A. Fidalgo-Marijuan, R. Gonçalves, M. M. Silva, S. Lanceros-Mendez, C.M. Costa, Lithium-ion battery separator membranes based on poly(L-lactic acid) biopolymer, Mater. Today Energy 18 (2020) 100494, https://doi.org/10.1016/j.mtener.2020.100494.
[68] R.F.P. Pereira, R. Brito-Pereira, R. Gonçalves, M.P. Silva, C.M. Costa, M.M. Silva, V. de Zea Bermudez, S. Lanceros-Méndez, Silk fibroin separators: a step toward lithium-ion batteries with enhanced sustainability, ACS Appl. Mater Interfaces 10 (6) (2018) 5385–5394, https://doi.org/10.1021/acsami.7b13802.
[69] A. Reizabal, A. Fidalgo-Marijuan, R. Gonçalves, A. Gutiérrez-Pardo, F. Aguesse, L. Pérez-Álvarez, J.L. Vilas-Vilela, C.M. Costa, S. Lanceros-Mendez, Silk fibroin and sericin polymer blends for sustainable battery separators, J. Colloid Interface Sci. 611 (2022) 366–376, https://doi.org/10.1016/j.jcis.2021.12.067.
[70] J.C. Barbosa, D.M. Correia, A. Fidalgo-Marijuan, R. Gonçalves, M. Fernandes, V. de Zea Bermudez, M.M. Silva, S. Lanceros-Mendez, C.M. Costa, Sustainable lithium-ion battery separators based on poly(3-Hydroxybutyrate-Co-Hydroxyvalerate) pristine and composite electrospun membranes, Energy Technol. 10 (2) (2022) 2100761, https://doi.org/10.1002/ente.202100761.
[71] J.P. Serra, A. Fidalgo-Marijuan, J. Teixeira, L. Hilliou, R. Gonçalves, K. Urtiaga, A. Gutiérrez-Pardo, F. Aguesse, S. Lanceros-Mendez, C.M. Costa, Sustainable lithium-ion battery separator membranes based on Carrageenan biopolymer, Adv. Sustain. Syst. 6 (12) (2022) 2200279, https://doi.org/10.1002/adsu.202200279.
[72] J.P. Serra, J. Uranga, R. Gonçalves, C.M. Costa, K. de la Caba, P. Guerrero, S. Lanceros-Mendez, Sustainable lithium-ion battery separators based on cellulose and soy protein membranes, Electrochim. Acta 462 (2023) 142746, https://doi.org/10.1016/j.electacta.2023.142746.
[73] J.P. Serra, J.C. Barbosa, M.M. Silva, R. Gonçalves, J. Uranga, C.M. Costa, P. Guerrero, K. de la Caba, S. Lanceros-Mendez, Wool/soy protein isolate membranes as separators toward more sustainable lithium-ion batteries, J. Energy Storage 75 (2024) 109748, https://doi.org/10.1016/j.est.2023.109748.
[74] S. Tchessalov, V. Maglio, P. Kazarin, A. Alexeenko, B. Bhatnagar, E. Sahni, E. Shalaev, Practical advice on scientific design of freeze-drying process: 2023 update, Pharm. Res. 40 (10) (2023) 2433–2455, https://doi.org/10.1007/s11095-023-03607-9.